

Supporting Information

Supporting Information Derivations of Equations

Error propagation

If D and f are estimated based on a b-value scheme with three b-values ($b_0 = 0$ and $b_1, b_2 > 0$), the variability of the parameter estimates can be calculated through error propagation (Eqs. 6 and 7). The derivations are outlined below.

$$\sigma_D^2 = \sum_{i=0}^2 \sigma_{S(b_i)}^2 \left(\frac{\partial D}{\partial S(b_i)} \right)^2 = \sum_{i=0}^2 \frac{\sigma^2}{n_i} \left(\frac{\partial}{\partial S(b_i)} \frac{\ln S(b_1) - \ln S(b_2)}{b_2 - b_1} \right)^2 = \sigma^2 \sum_{i=1}^2 \frac{1}{n_i} \left(\frac{1}{b_2 - b_1} \frac{1}{S_0(1-f)e^{-b_i D}} \right)^2 \quad (S1)$$

$$\begin{aligned} \sigma_f^2 &= \sum_{i=0}^2 \sigma_{S(b_i)}^2 \left(\frac{\partial f}{\partial S(b_i)} \right)^2 = \sigma^2 \sum_{i=0}^2 \frac{1}{n_i} \left(\frac{\partial}{\partial S(b_i)} \left[1 - \frac{1}{S(b_0)} \left(\frac{S(b_1)^{b_2}}{S(b_2)^{b_1}} \right)^{\frac{1}{b_2 - b_1}} \right] \right)^2 = \\ &= \sigma^2 \left\{ \frac{1}{n_0} \left(\frac{1-f}{S_0} \right)^2 + \frac{1}{S_0^2 (b_2 - b_1)^2} \left[\frac{1}{n_1} (b_2 e^{b_1 D})^2 + \frac{1}{n_2} (b_1 e^{b_2 D})^2 \right] \right\} \quad (S2) \end{aligned}$$

The noise level for a given b-value is assumed to depend only on the number of acquisition of the particular b-value, i.e. $\sigma_{S(b_i)}^2 = \sigma^2/n_i$. The derivations were performed by inserting the closed form solution of the particular parameter, evaluating the partial derivative and then use the signal model (Eq. 2).

Elements of the Fisher matrix

The elements of the Fisher matrix are composed of combinations of partial derivatives as shown in Equation 8. These partial derivatives are:

$$\frac{\partial S(b_i)}{\partial D} = -b_i S_0 (1-f) e^{-b_i D} \quad (S3)$$

$$\frac{\partial S(b_i)}{\partial f} = -S_0 [e^{-b_i D} - \delta(b_i)] \quad (S4)$$

$$\frac{\partial S(b_i)}{\partial S_0} = (1-f) e^{-b_i D} + f \delta(b_i) \quad (S5)$$

TE-related SNR penalty

The signal at $b = 0$ (S_0) measured at echo time TE is a weighted average based on the characteristics of the two compartments:

$$S_0 = S_{00} \left((1 - f_0) e^{-\frac{TE}{T_2^d}} + f_0 e^{-\frac{TE}{T_2^p}} \right) \quad (S6)$$

where f_0 is the size of the perfusion compartment when adjusting for transverse relaxation and S_{00} is the signal without diffusion weighting and $TE = 0$. As shown by Jerome et al.³², the f that is estimated without considering relaxation effects is:

$$f = f_0 e^{-\frac{TE}{T_2^p}} \left((1 - f_0) e^{-\frac{TE}{T_2^d}} + f_0 e^{-\frac{TE}{T_2^p}} \right)^{-1} \quad (S7)$$

i.e. the fraction of signal from the perfusion compartment relative to the total signal. The inverse of Equation S7 is:

$$f_0 = f e^{-\frac{TE}{T_2^d}} \left((1 - f) e^{-\frac{TE}{T_2^p}} + f e^{-\frac{TE}{T_2^d}} \right)^{-1} \quad (S8)$$

If Equation S8 is inserted into Equation S6, the result is:

$$S_0 = S_{00} e^{-TE \left(\frac{1}{T_2^d} + \frac{1}{T_2^p} \right)} \left((1 - f) e^{-\frac{TE}{T_2^p}} + f e^{-\frac{TE}{T_2^d}} \right)^{-1} \quad (S9)$$

which shows the penalty factor used in the b-value optimization.

Supporting Information Tables

Supporting Information Table S1. As table 1, but without an upper b-value limit. Optimal number of acquisitions of each optimal b-value for different total number of acquisitions (n_{tot}) and the proportions for the limiting case of an infinite total number of acquisitions. The optimal b-values were $b_0 = 0$, $b_1 = 200 \text{ s/mm}^2$ and b_2 as shown in the table

n_{tot}	3	4	5	6	7	8	9	10	11	12	∞
n_0	1	1	1	1	1	2	2	2	2	2	19 %
n_1	1	2	2	3	3	3	4	4	5	5	43 %
n_2	1	1	2	2	3	3	3	4	4	5	38 %
$b_2 \text{ [s/mm}^2\text{]}$	886	855	860	838	838	872	857	860	847	849	854

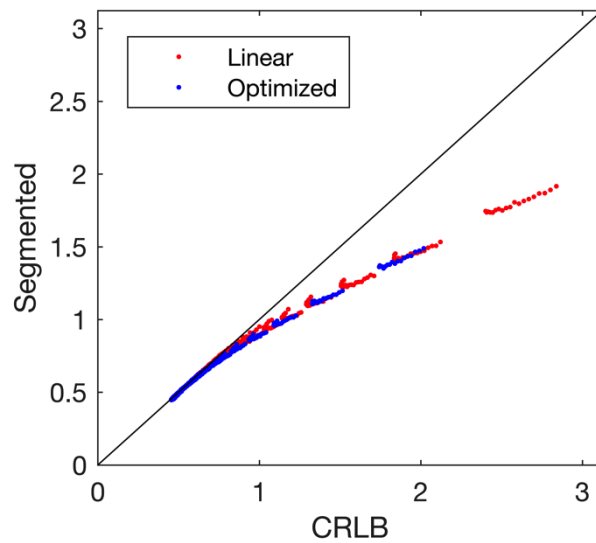
Supporting Information Table S2. As table 1, but without the correction for changes on the echo time (see detailed description in caption for Table 1 or Supporting Table S1). The optimal b-values were $b_0 = 0$, $b_1 = 200$ and $b_2 = 800 \text{ s/mm}^2$

n_{tot}	3	4	5	6	7	8	9	10	11	12	∞
n_0	1	1	1	1	1	2	2	2	2	2	19 %
n_1	1	2	2	3	3	3	4	4	5	5	43 %
n_2	1	1	2	2	3	3	3	4	4	5	38 %

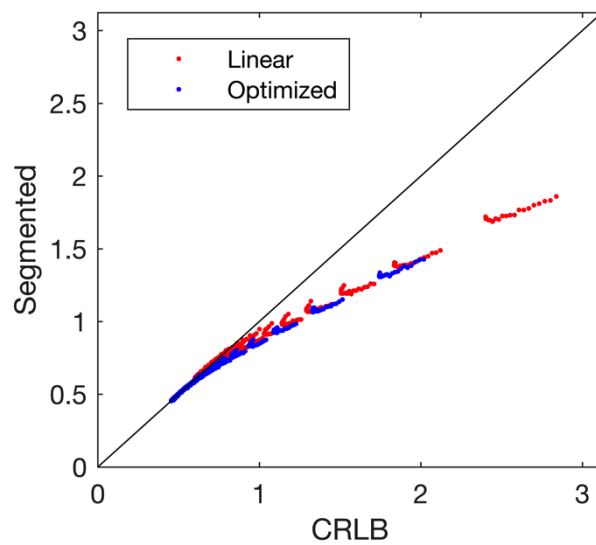
Supporting Information Table S3. As table 1, but with neither an upper b-value limit nor a correction for changes on the echo time (see detailed description in caption for Table 1 or Supporting Table S1). The optimal b-values were $b_0 = 0$, $b_1 = 200 \text{ s/mm}^2$ and b_2 as shown in the table

n_{tot}	3	4	5	6	7	8	9	10	11	12	∞
n_0	1	1	1	1	1	2	2	2	2	2	20 %
n_1	1	1	2	2	3	3	3	4	4	5	39 %
n_2	1	2	2	3	3	3	4	4	5	5	40 %
$b_2 \text{ [s/mm}^2\text{]}$	1299	1399	1294	1347	1290	1297	1334	1294	1322	1292	1297

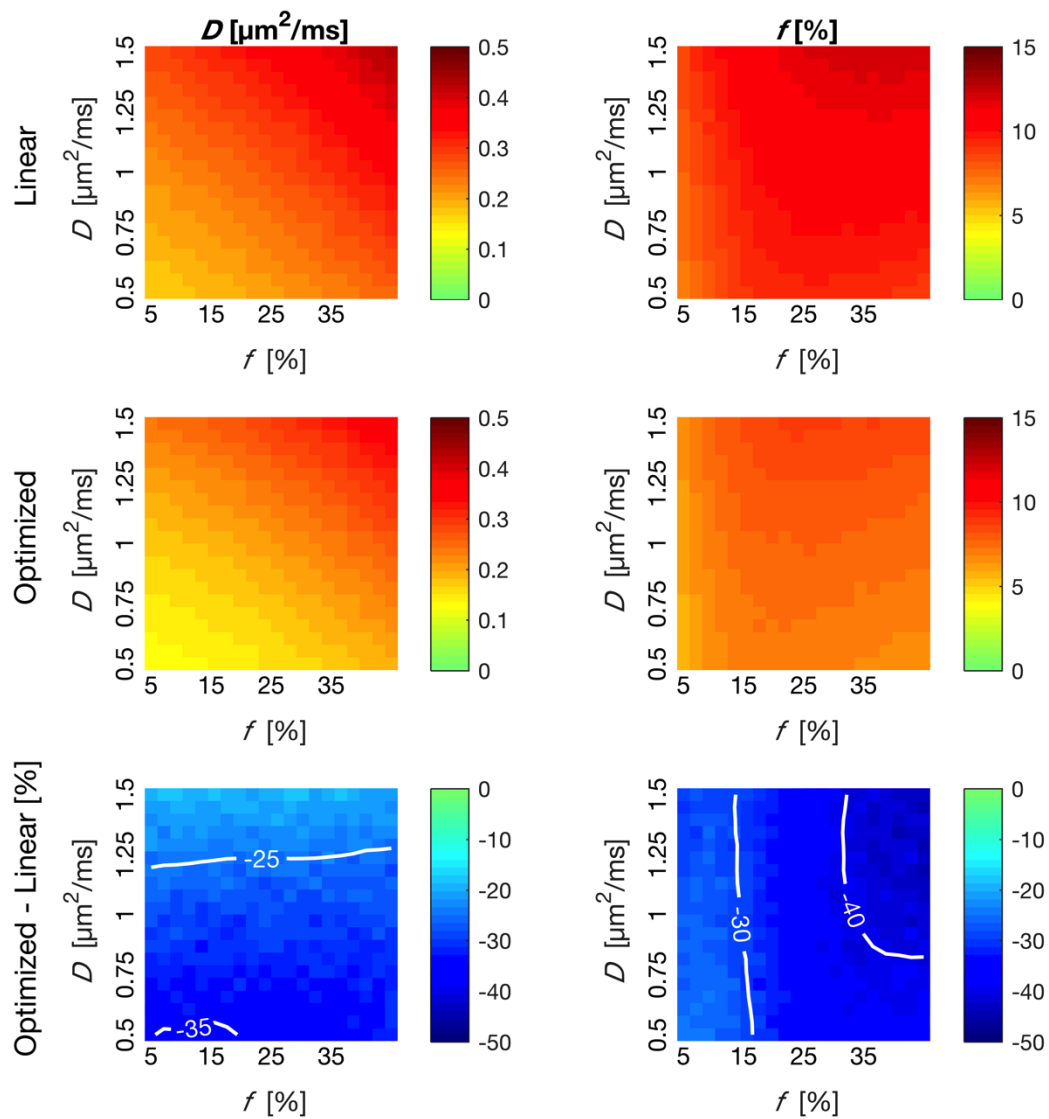
Supporting Information Figures



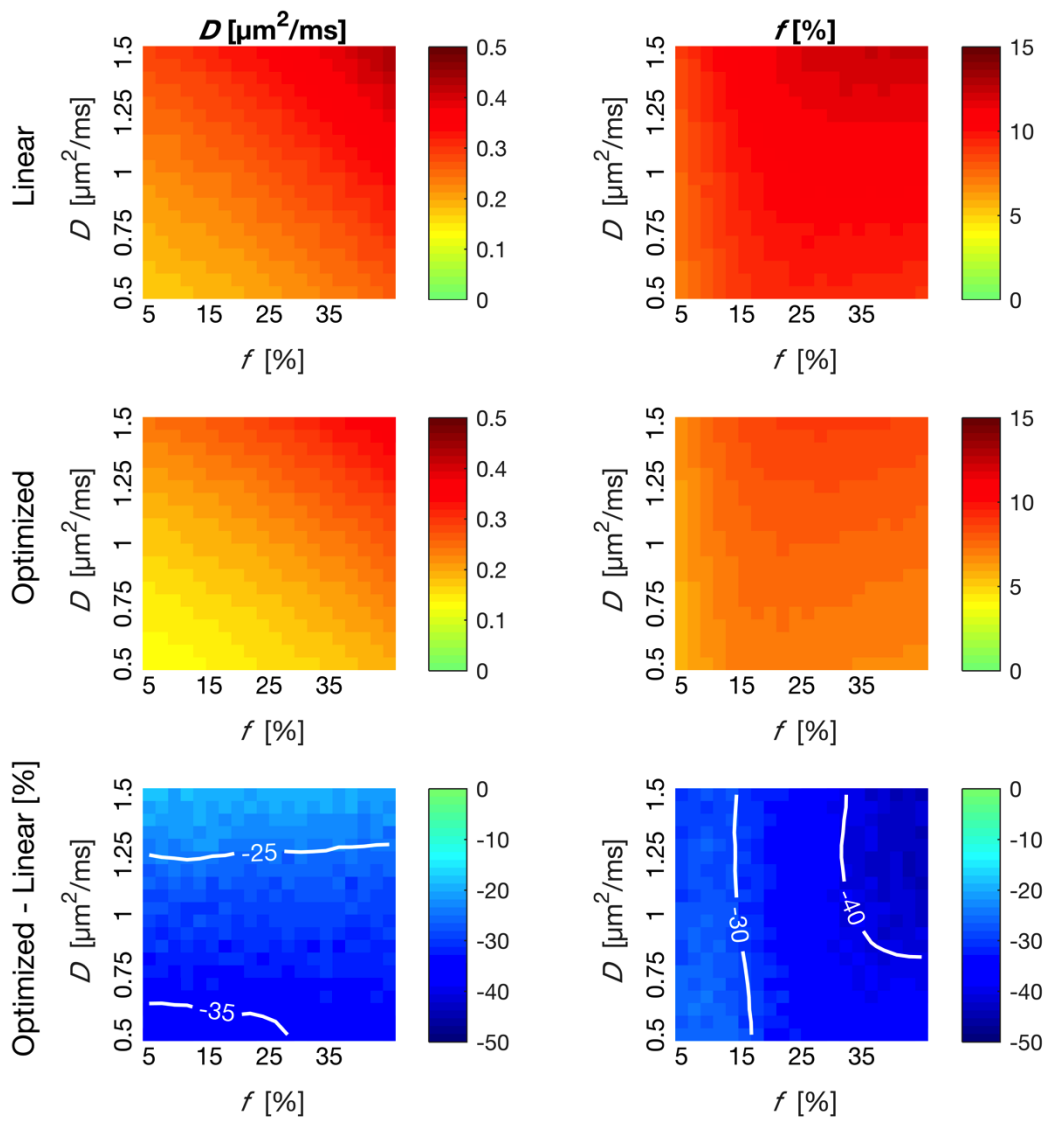
Supporting Information Figure S1. As Figure 1, but with $D^* = 20 \mu\text{m}^2/\text{ms}$. Comparison between estimation variability based on CRLB and segmented model fitting based on simulated data. The red and blue markers show results based on the linear and optimized b-value schemes respectively. Each data point represents the total relative error (Eq. 11 or its equivalent measure derived from segmented model fitting) for a given combination of D and f . The line of unity is shown in black.



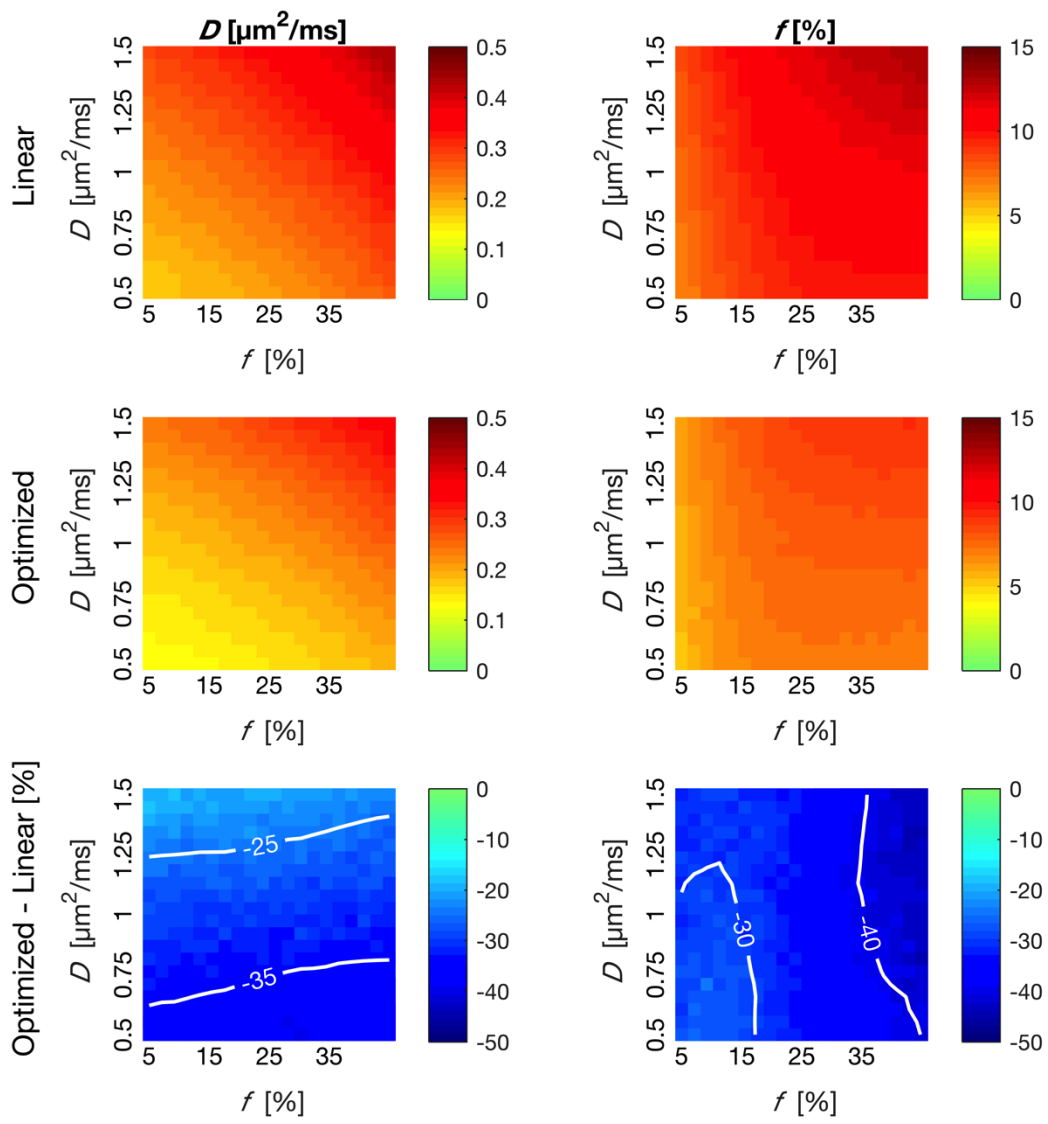
Supporting Information Figure S2. As Figure 1, but with $D^* = 10 \mu\text{m}^2/\text{ms}$ (see detailed description in caption for Figure 1 or Supporting Figure S1)



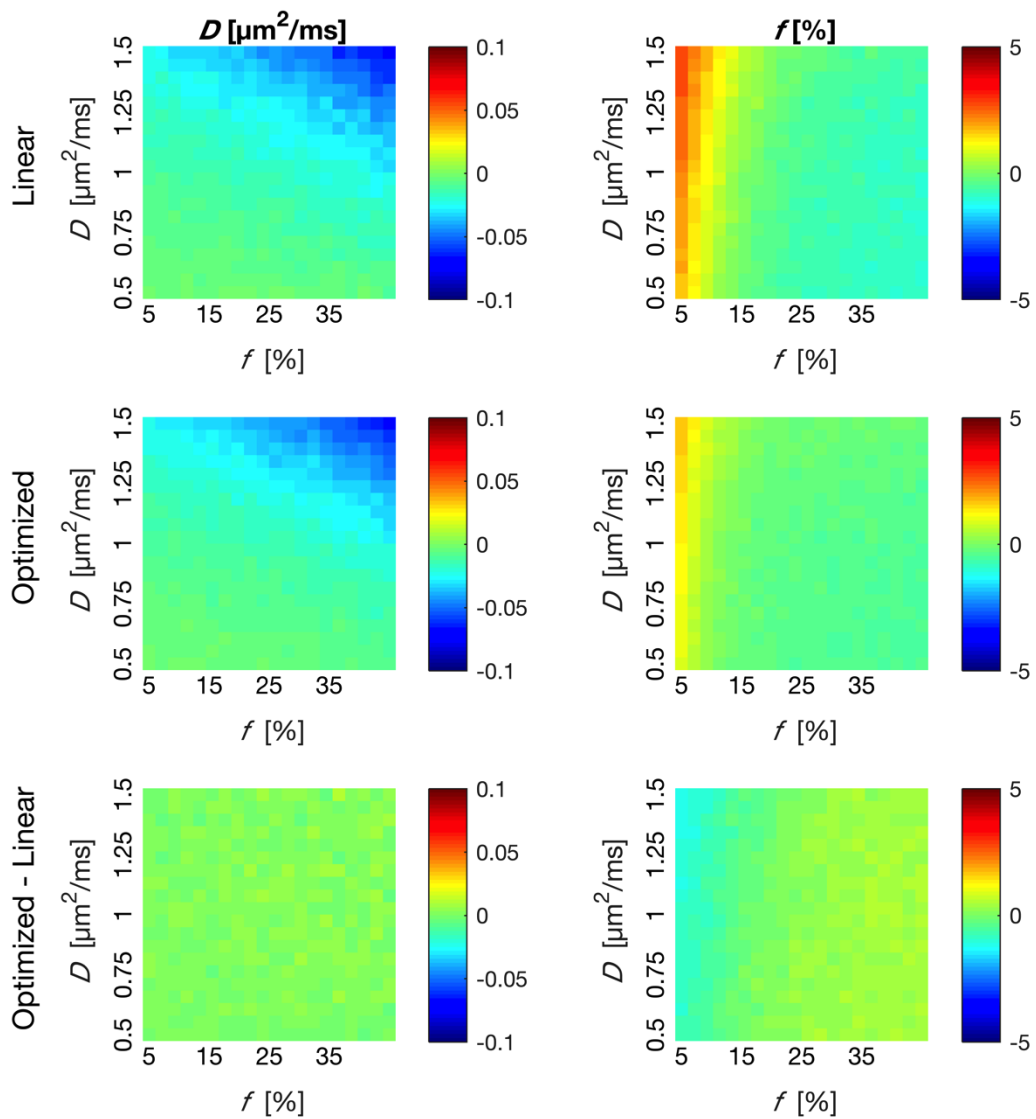
Supporting Information Figure S3. Each column shows the standard deviation of parameter estimates obtained from simulations at each combination of D and f , for each b-value scheme and their relative difference. The bottom plots are the same as those shown in Figure 2. Data were generated with $D^* = 50 \mu\text{m}^2/\text{ms}$



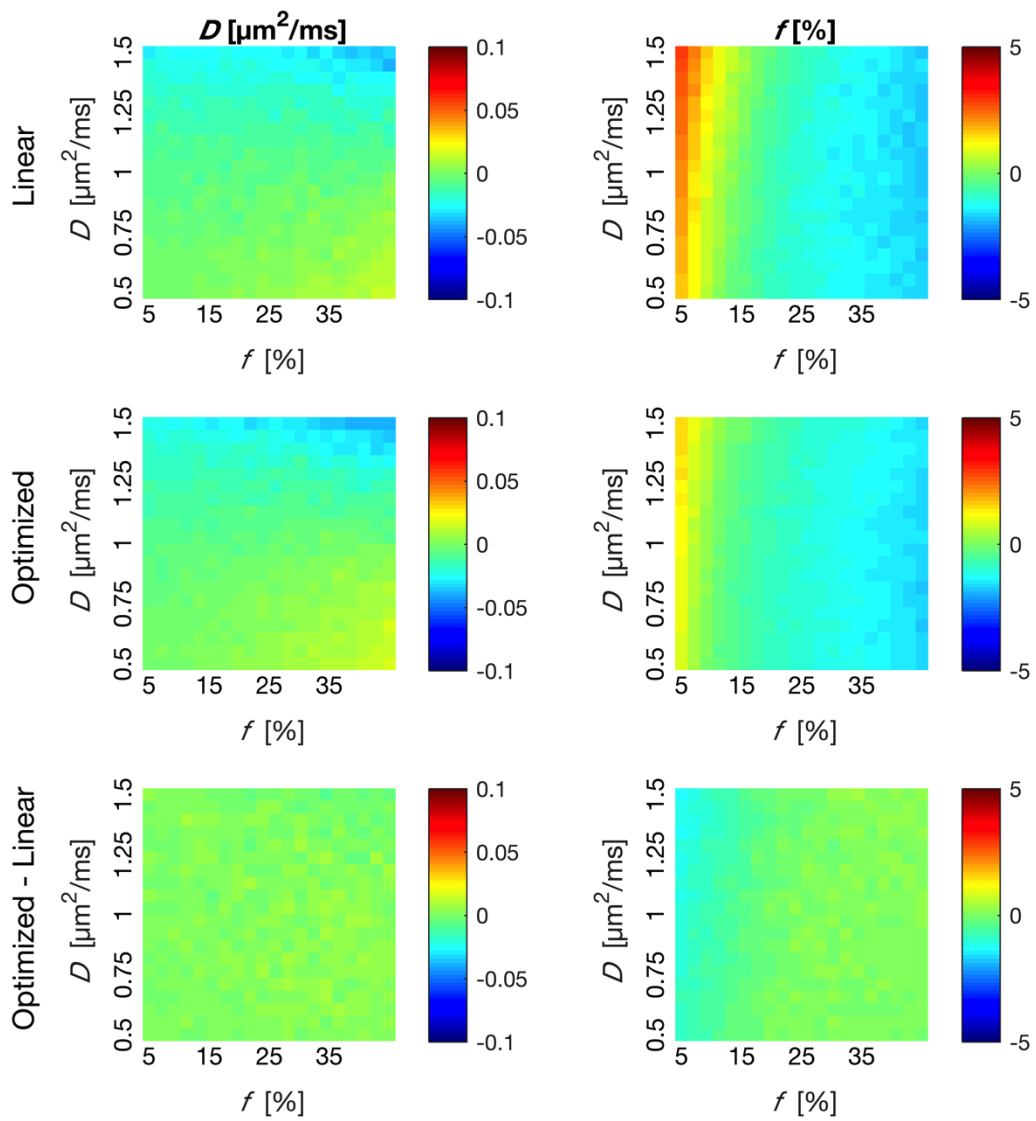
Supporting Information Figure S4. As Supporting Figure S3, but with $D^* = 20 \mu\text{m}^2/\text{ms}$



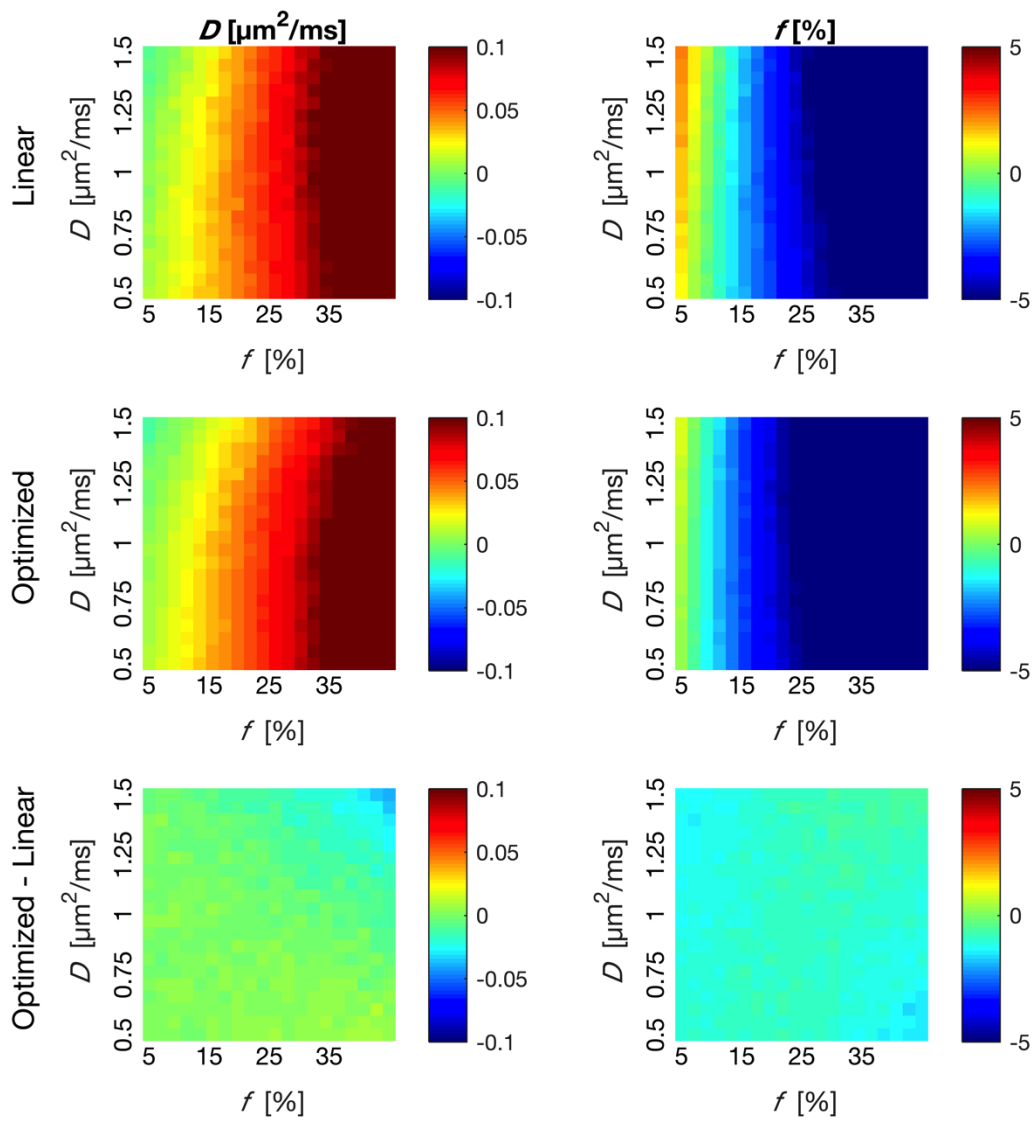
Supporting Information Figure S5. As Supporting Figure S3, but with $D^* = 10 \mu\text{m}^2/\text{ms}$



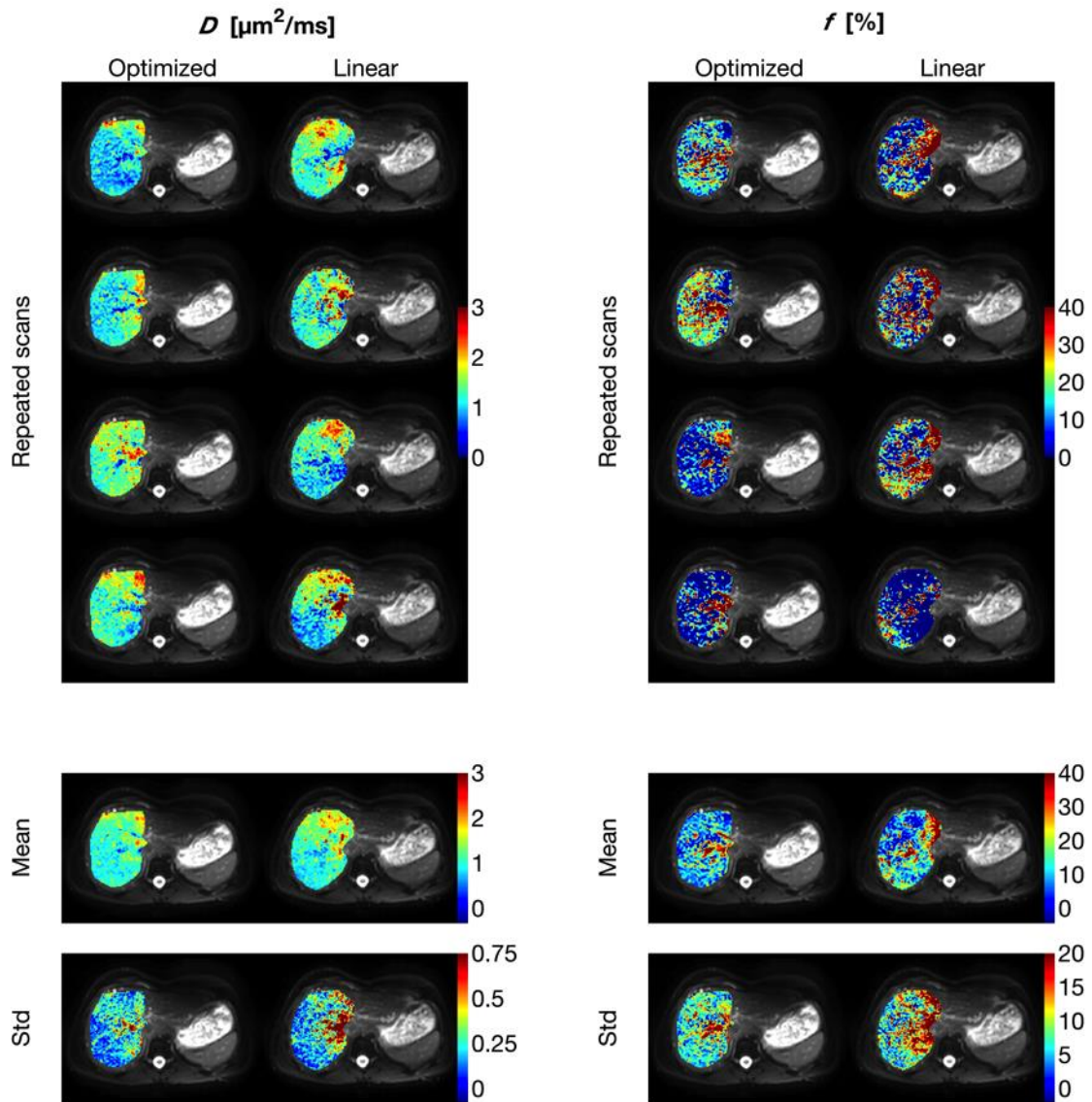
Supporting Information Figure S6. Each column shows the mean difference between parameter estimates obtained from simulations and their true value at each combination of D and f , for each b-value scheme and their difference. The data shown in the upper two rows of plots are the same as what is used in Figure 3, but the dependence on D is also shown in this figure. Data were generated with $D^* = 50 \mu\text{m}^2/\text{ms}$



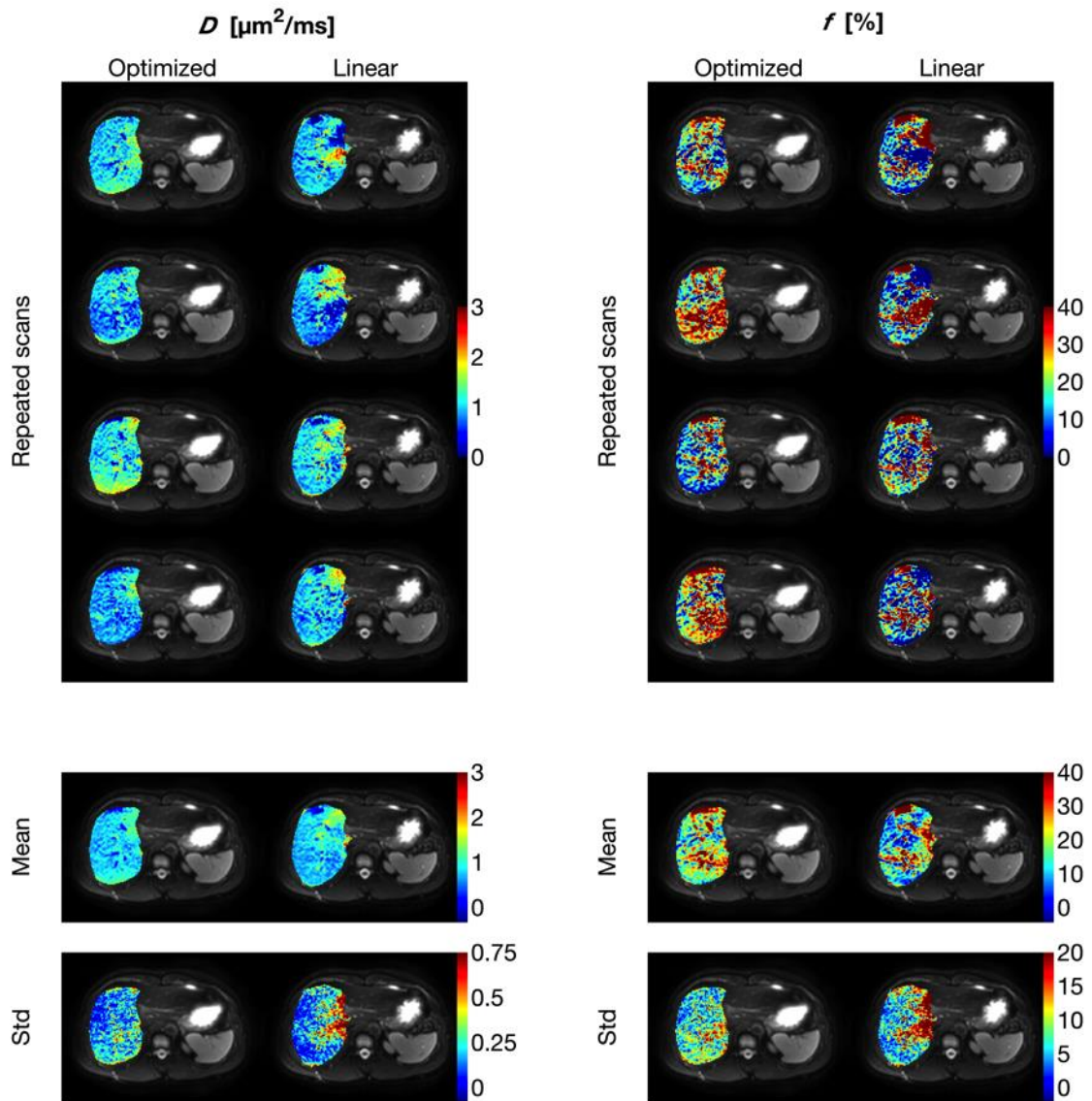
Supporting Information Figure S7. As Supporting Figure S6, but with $D^* = 20 \mu\text{m}^2/\text{ms}$



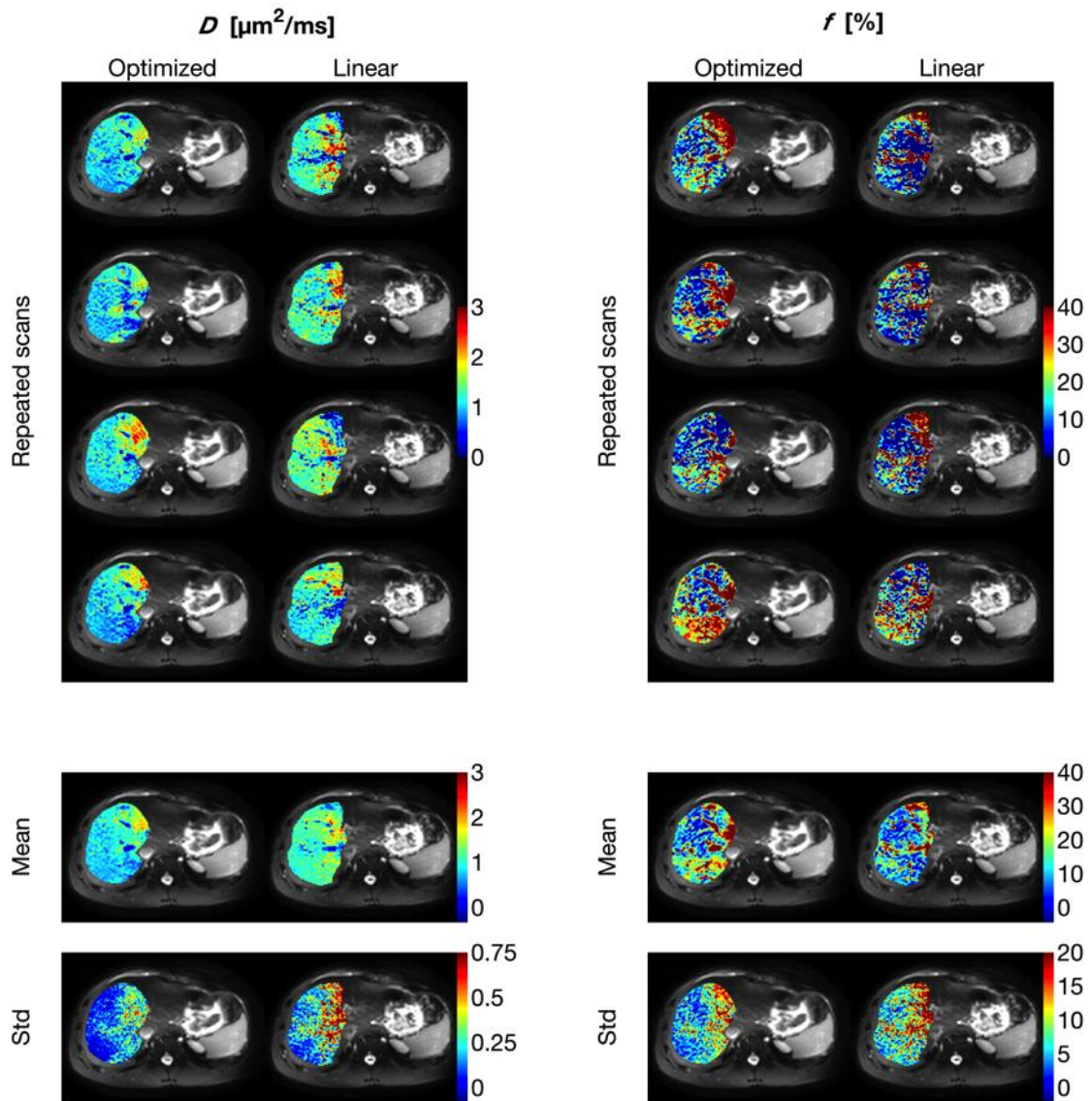
Supporting Information Figure S8. As Supporting Figure S6, but with $D^* = 10 \mu\text{m}^2/\text{ms}$



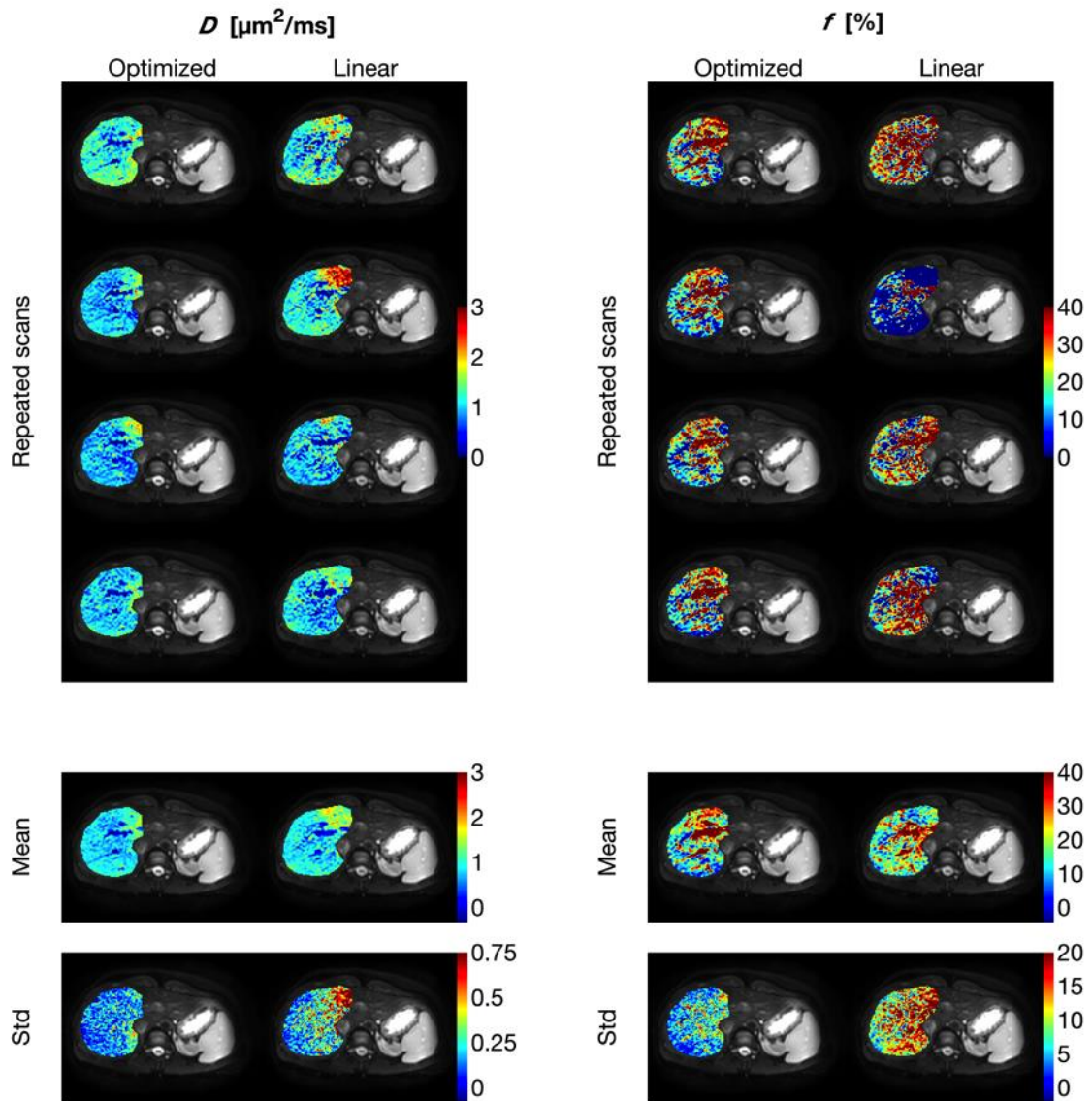
Supporting Information Figure S9. Parameter maps (color) of the right part of the liver superimposed on the $b = 0$ image (gray scale) from an example subject. The figure shows parameter maps from repeated scans as well as the mean and the standard deviation of those maps. As Figures 5 and 6, but different subject



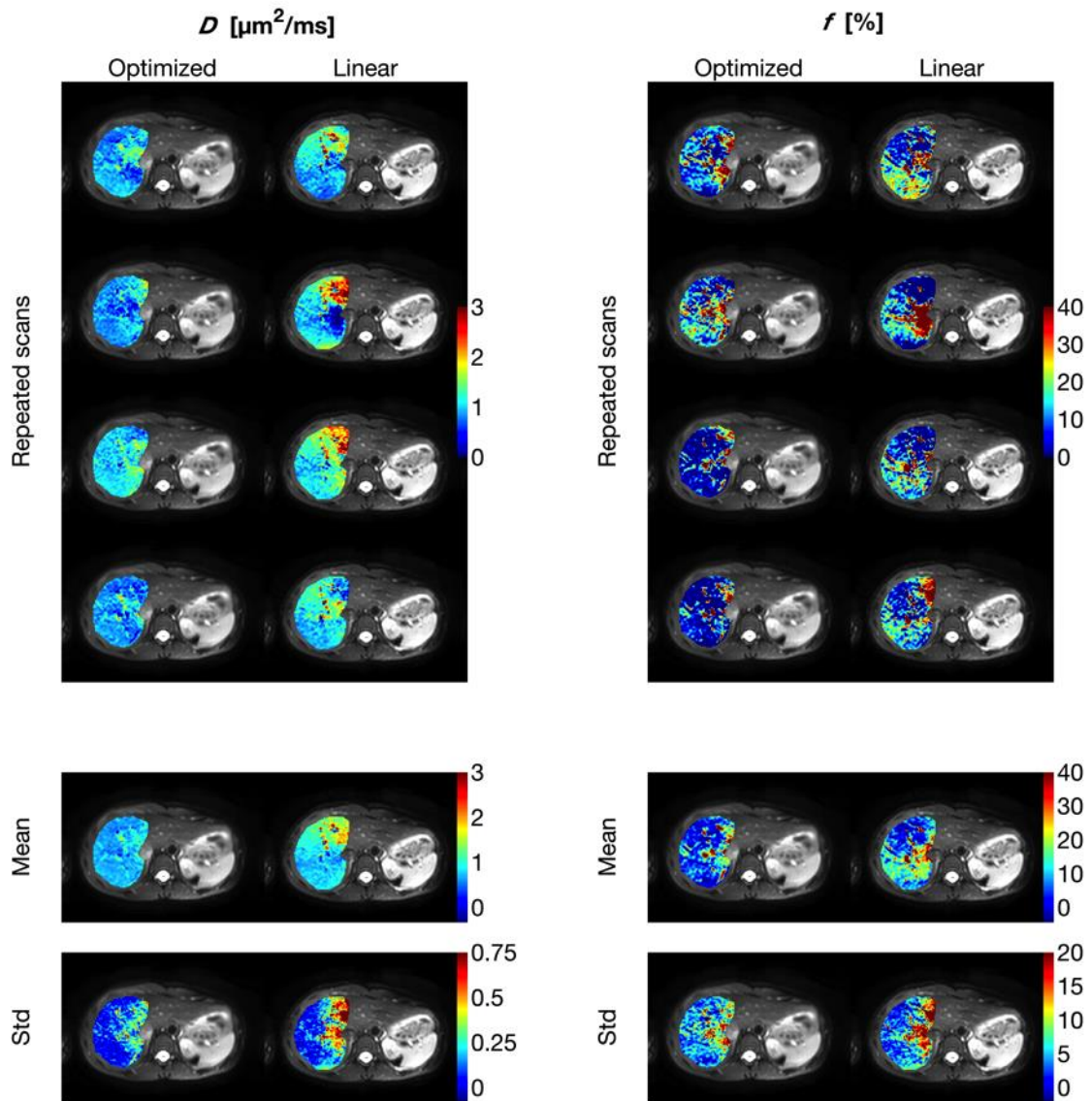
Supporting Information Figure S10. As Figures 5 and 6, but different subject (see caption for Figures 5 and 6, or Support Figure S9 for detailed description)



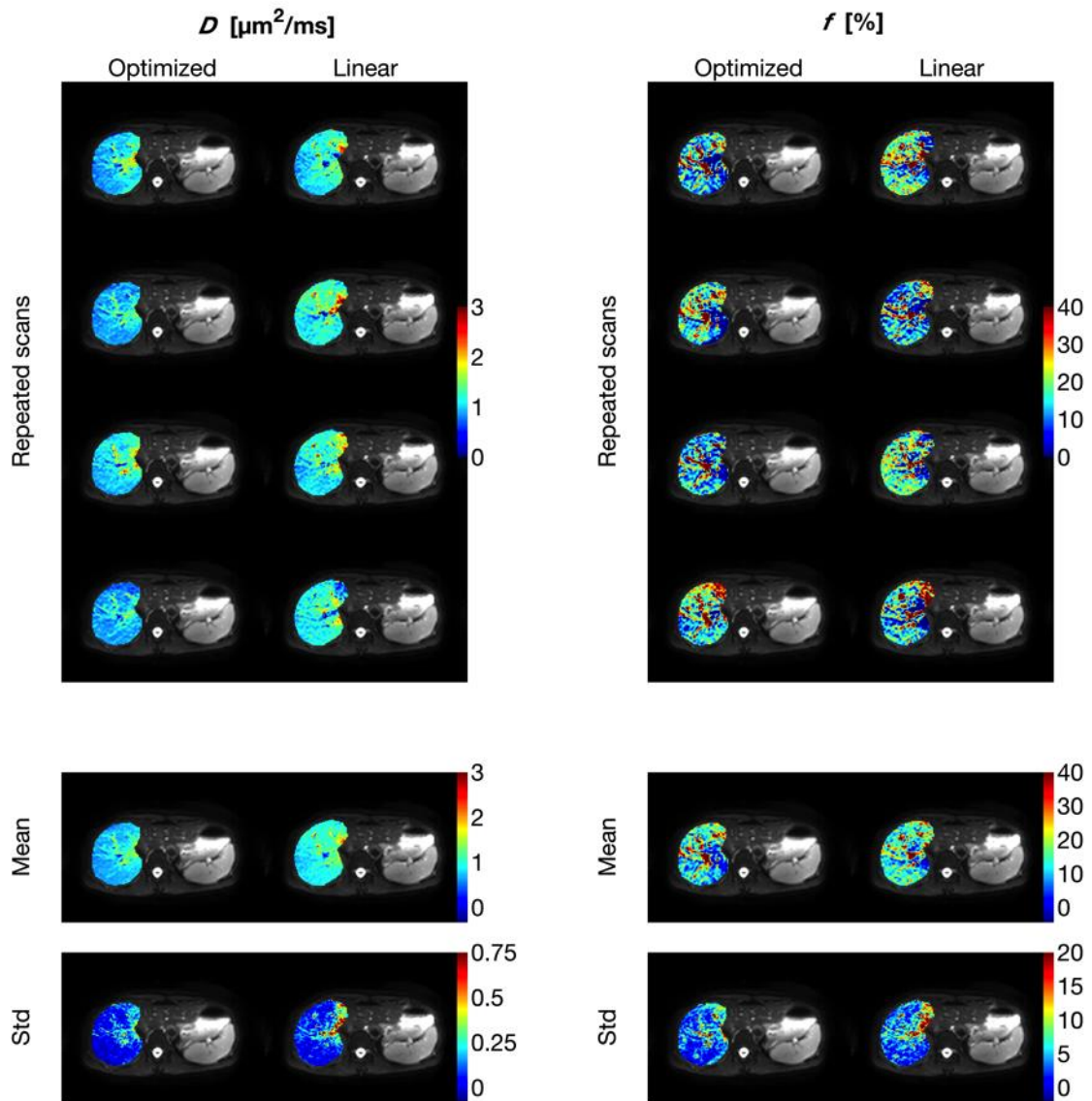
Supporting Information Figure S11. As Figures 5 and 6, but different subject (see caption for Figures 5 and 6, or Support Figure S9 for detailed description)



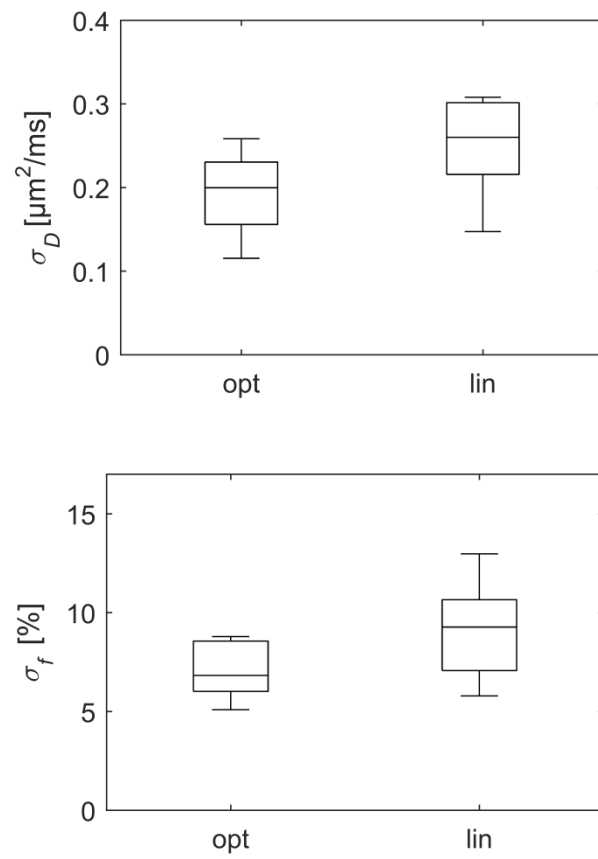
Supporting Information Figure S12. As Figures 5 and 6, but different subject (see caption for Figures 5 and 6, or Support Figure S9 for detailed description)



Supporting Information Figure S13. As Figures 5 and 6, but different subject (see caption for Figures 5 and 6, or Support Figure S9 for detailed description)



Supporting Information Figure S14. As Figures 5 and 6, but different subject (see caption for Figures 5 and 6, or Support Figure S9 for detailed description)



Supporting Information Figure S15. Median standard deviation of parameter estimates over repeated measurements for each subject and b-value scheme